Scientific African 32 (2026) e03416

Contents lists available at ScienceDirect

Scientific African

journal homepage: www.elsevier.com/locate/sciaf

Modelling deforestation, carbon stock changes, and identification of optimal forest restoration sites in a rapidly urbanising landscape

Nobert Tafadzwa Mukomberanwa *, Talent Kamanga, Blessing Onias Munetsi

Department of Geoinformatics and Environmental Conservation, Chinhoyi University of Technology, P. Bag 7724, Chinhoyi, Zimbabwe

ARTICLE INFO

Editor: Mohamed Fathy El-Amin Mousa

Keywords:
Deforestation
Carbon stocks
Restoration sites
Machine learning

ABSTRACT

Developing towns and cities worldwide face high deforestation rates, yet accurate information on its spatial extent, dynamics, and potential restoration sites remains limited. Forest ecosystems play a pivotal role in carbon sequestration; however, their degradation disrupts ecological functions, necessitating spatially explicit assessments of carbon stock changes over time. Understanding the spatiotemporal patterns of forest loss is essential for assessing carbon dynamics and guiding targeted restoration interventions across ecologically sensitive and socio-economically vulnerable landscapes. This study aimed to assess deforestation dynamics, quantify forest cover, and identify potential restoration sites in Chinhoyi, Zimbabwe. Using Geographical Information Systems (GIS), Remote Sensing (RS), and the Random Forest (RF) machine learning algorithm, the study assessed forest cover loss and restoration suitability. Potential restoration sites were identified by evaluating factors such as slope, proximity to roads and settlements, and land use land cover (LULC) patterns using the Weighted Overlay Analysis (WOA) and Analytical Hierarchy Process (AHP). Findings revealed a 54.58 % net reduction in forest cover from 2014 to 2024, largely driven by agricultural expansion, urbanization, and land degradation. However, transition analysis also indicated localized regeneration, with 4.57 %–15.17 % ha of forest gains observed in different intervals, highlighting natural regrowth and reforestation processes. Carbon stock analysis indicated significant losses, with 45,252 tons of carbon emissions exceeding regional averages over the decade. The study recommends prioritizing reforestation and forest restoration efforts in highly suitable areas to recover forest cover and mitigate the impacts of continued deforestation.

Introduction

Natural ecosystems are critical to human well-being due to the essential goods and services they provide, including food production, carbon sequestration, and water regulation [1]. The sustainability of these services hinges on maintaining a balance between socioeconomic development and environmental conservation [2]. However, over the past five decades, human activities have driven rapid and extensive ecosystem modifications, especially through land-use changes [3]. The earth has entered the Anthropocene epoch where humans are now dominating the system earth. These transformations, while promoting economic development, have often come at the cost of degrading vital ecosystem functions [4]. Deforestation, in particular, has drastically reshaped landscapes, contributing to biodiversity loss, disrupted hydrological cycles, and increased carbon emissions [5]. Spatial and temporal patterns of

* Corresponding author.
E-mail address: nobertmukomberanwa@gmail.com (N.T. Mukomberanwa).

https://doi.org/10.1016/j.sciaf.2026.e03416
Received 19 July 2025; Received in revised form 7 May 2026; Accepted 16 May 2026
Available online 18 May 2026

forest loss are highly variable, influenced by regional drivers such as agricultural expansion, urban growth, illegal logging, and infrastructure development [2]. In Africa, population growth has exacerbated the trade-offs between food production and ecosystem conservation, accelerating forest degradation [3]. According to FAO's Global Forest Resources Assessments (FRA), global forest area has continued to decline, although the rate of net loss has slowed in recent decades. While some regions (e.g., Europe, East Asia) have experienced forest gains due to reforestation and afforestation programs, these do not offset the persistent large-scale losses in tropical developing regions. The spatial configuration of forests, not just their extent, plays a crucial role in maintaining ecosystem functionality [6]. Fragmentation and degradation of forested landscapes have impaired ecological processes such as erosion control, nutrient cycling, and climate regulation [7]. These challenges have intensified, emphasizing the need for spatially informed conservation strategies to safeguard ecosystem services and biodiversity.

Chinhoyi, a rapidly expanding urban centre in north-central Zimbabwe, has experienced significant land use and land cover transformations over the past decade, largely driven by urban growth, agricultural expansion, and deforestation. The area represents a critical environmental transition zone between urban and rural landscapes, making it an ideal case for assessing deforestation dynamics, carbon loss, and opportunities for ecological restoration. Chinhoyi was selected as the case study area due to its diverse land cover types, increasing anthropogenic pressures, and the availability of high-quality spatial data suitable for machine learning and RS analysis. Natural forests serve as vital carbon sinks within terrestrial ecosystems, playing a central role in mitigating global climate change [6]. However, ongoing anthropogenic degradation, including deforestation and land-use change, continues to reduce their capacity to store carbon [8]. Understanding the spatiotemporal dynamics of carbon stocks is essential for assessing forest contributions to the global carbon cycle and informing effective climate mitigation policies [9]. LULC significantly influence carbon storage by altering vegetation biomass and soil carbon pools [7]. These transformations are driven by both natural disturbances—such as wildfires, storms, and insect outbreaks—and anthropogenic activities including logging, agricultural expansion, grazing, and urbanization [10]. The impact of LULC on forest carbon dynamics varies across regions and management intensities [11]. For instance, studies from tropical forests in Mexico have shown that areas with lower management intensity tend to have higher aboveground carbon stocks [12]. According to the environmental Kuznets curve hypothesis, rising incomes may reduce deforestation pressure, whereas rural poverty can exacerbate forest degradation due to unsustainable resource use [13]. In some cases, agricultural abandonment following urbanization has led to forest regeneration, suggesting socio-economic factors are critical in shaping land-use trajectories [14]. Given the urgency of meeting international climate targets such as those outlined in the Paris Agreement and Kyoto Protocol, accurate monitoring of forest carbon dynamics is imperative [15]. Reliable methods include the use of periodic forest inventories, allometric equations, and spatial modelling to estimate carbon stock changes [16]. Recent studies highlight the importance of integrating spatiotemporal analyses of land-use changes with forest management strategies to enhance carbon sequestration [17,4,2].

Improving forest structure for carbon storage is essential for mitigating climate change [5]. Ecological restoration, particularly through forest landscape restoration (FLR), has emerged as a key strategy to reverse land degradation and enhance ecosystem sustainability [12]. Restoration efforts aim to re-establish ecosystem functionality, yet the spatiotemporal patterns and contributions of ecological restoration spaces (ERS) to ecosystem services remain underexplored. Given the global decline of forests due to synergistic anthropogenic and natural drivers, prioritizing restoration sites has become increasingly important [18]. Resource constraints necessitate targeted interventions, focusing active restoration on highly degraded sites while allowing passive regeneration in areas with higher natural recovery potential [19]. Active restoration refers to deliberate human interventions aimed at accelerating the recovery of degraded forest ecosystems. This may include tree planting, soil and water conservation measures, enrichment planting, or assisted natural regeneration through selective weeding and protection. Passive regeneration (also called natural regeneration) refers to the spontaneous recovery of forest cover without direct planting or intensive human intervention, often occurring when disturbances such as logging, fire, or cultivation are halted and ecological processes are allowed to restore vegetation naturally [20]. Evidence from Santa Cruz Island (California, USA) illustrates restoration success, with carbon sequestration increasing by 97 % following the removal of grazing ungulates [14]. Such cases highlight the ecological benefits of site-specific interventions [10]. However, restoration success depends on appropriate site selection, which must consider degradation levels, ecological criteria, and landscape-scale functionality [1]. Traditional projects have sometimes targeted excessively degraded areas, whereas a more effective approach involves integrating restoration efforts within protected areas where ecological integrity can be more feasibly maintained [17]. Secondary tropical forests, although disturbed, remain critical for timber, non-timber products, and biodiversity conservation [21]. Their sustainable management requires nuanced understanding of site productivity, species composition, and forest structure [22]. Restoration strategies such as reforestation and afforestation have shown varying outcomes depending on site characteristics, and success is strongly influenced by spatial planning and environmental suitability [23]. Nevertheless, criteria and indicators (C&I) for prioritization remain underdeveloped, especially those suitable for spatial analysis across diverse ecological and socio-economic contexts [24]. FLR provides a broader approach by aiming to restore multiple forest functions at the landscape level while supporting human well-being [25]. Identifying restoration areas requires combining historical landscape assessments with current ecological functionality to optimize outcomes [3]. The Bonn Challenge and similar global commitments underscore the urgency of restoring large-scale degraded lands [23]. Frameworks developed by organizations such as International Union for Conservation of Nature (IUCN) and World Resources Institute (WRI) guide national-level assessments, including economic evaluations and multi-stakeholder involvement [26]. Rwanda provides a leading example of spatially identifying restoration opportunities using these frameworks [27–29]. At the regional level, restoration site selection methods have increasingly integrated landscape ecology, historical data, and modelling techniques such as multi-criteria analysis, ecological zoning, and machine learning [30].

Accurate detection of forest change is essential for understanding long-term environmental dynamics and supporting effective forest management and conservation policies [31]. Producing reliable, detailed, and continuous spatial data over large areas enables

better monitoring of forest degradation and carbon stock changes [3]. High-quality forest maps are crucial for informing decision-making related to reforestation, rehabilitation, and sustainable landscape management [31]. With increasing deforestation driven by natural and anthropogenic disturbances, identifying and prioritizing sites for ecological restoration has become a global imperative [32]. Advancements in RS technologies and open-access satellite data have revolutionized environmental monitoring [11]. Modern Earth observation platforms now offer high resolution spatial, spectral, and temporal data that allow for near real-time tracking of deforestation and associated ecosystem changes [12]. Field-based carbon estimation methods, such as destructive

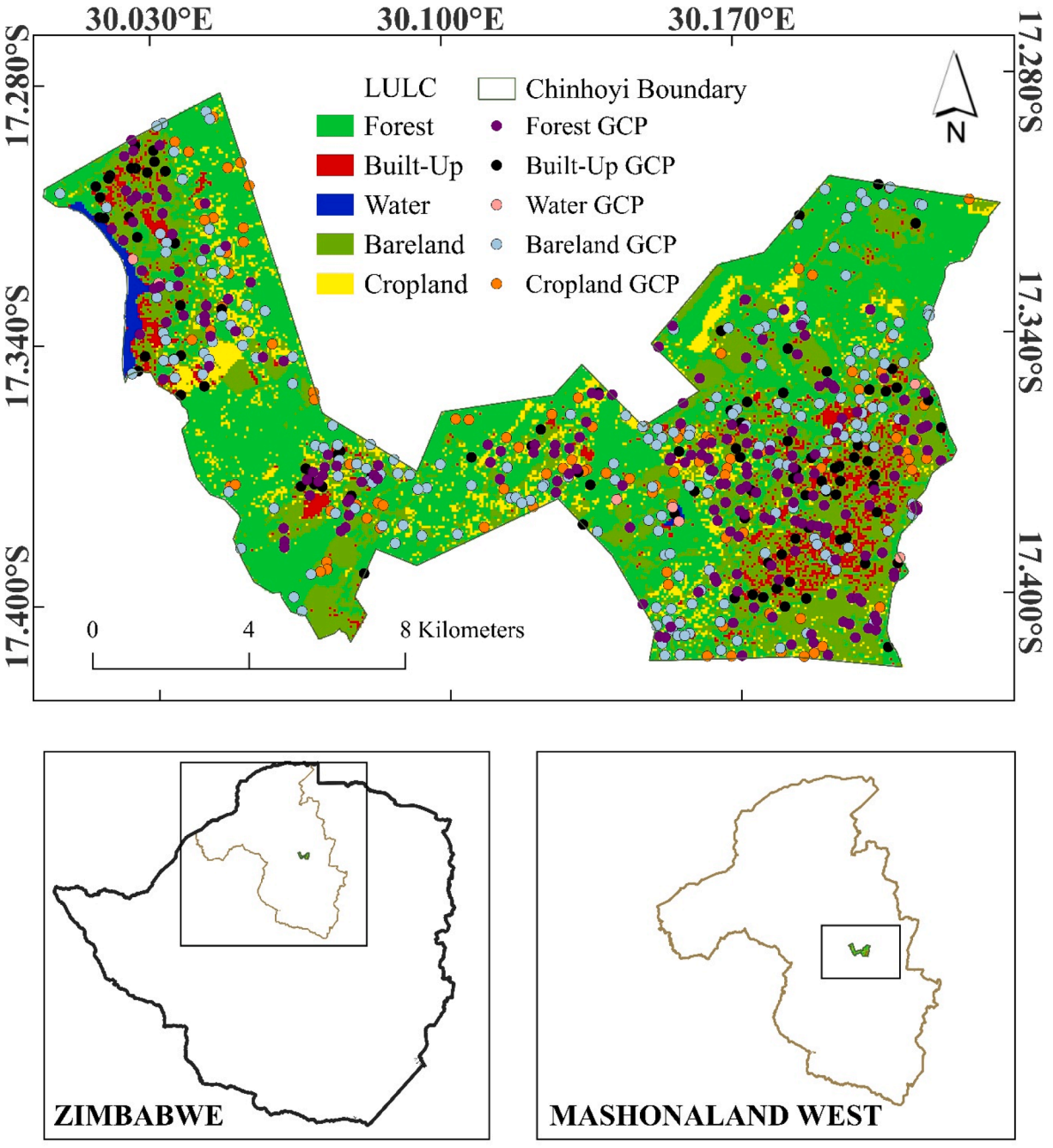

Fig. 1. Study area and land use/land cover distribution of Chinhoyi, Zimbabwe. Spatial distribution of land use/land cover (LULC) classes within the Chinhoyi municipal boundary, including forest, built-up areas, water, bareland, and cropland, derived from satellite-based classification. Overlaid points represent ground control points (GCPs) used for accuracy assessment, stratified by LULC class. Geographic coordinates are provided in degrees (WGS 84), with a scale bar indicating distance in kilometres and a north arrow for orientation. Insets show the location of the study area within Zimbabwe and the Mashonaland West Province, respectively.

biomass sampling, though accurate, are often labour-intensive, time-consuming, and impractical for large-scale forest monitoring [5]. As a result, integrating field measurements with RS data provides a more efficient and spatially explicit approach to estimating forest biomass and carbon stocks [14]. Numerous studies have demonstrated the utility of RS in supporting carbon inventories by combining satellite observations with ground truth data to assess carbon distribution across forest ecosystems [33,34,24]. Despite growing interest in forest restoration, determining optimal sites for intervention remains complex due to the need to account for ecological, biophysical, and socio-economic variables [13]. Recent methodological advances—such as spatial multi-criteria analysis (SMCA), machine learning, and ecological modelling—have improved the ability to synthesize diverse datasets and assess restoration feasibility [3].

This study aims to examine the spatiotemporal dynamics of deforestation and carbon stock changes between 2014 and 2024, with a focus on identifying optimal forest restoration areas. Specifically this study aimed to (i) determine the spatial and temporal dynamics of deforestation in Chinhoyi from 2014 to 2024 using the RF machine learning algorithm, GIS, and multitemporal satellite imagery (ii) estimate carbon stocks lost to deforestation in Chinhoyi from 2014 to 2024 using Above Ground Biomass (AGB) and quantify carbon dioxide emissions from deforestation and (iii) identify optimal sites for vegetation restoration in Chinhoyi using GIS and RS, considering land cover, soil type, proximity to roads and settlements, and elevation. The research questions were: (i) How have the spatial and temporal patterns of deforestation in Chinhoyi evolved between 2014 and 2024 as detected using the RF algorithm, GIS, and multitemporal satellite imagery? (ii) What is the estimated amount of carbon stock lost and corresponding carbon dioxide emissions resulting from deforestation in Chinhoyi between 2014 and 2024? (iii) Which areas in Chinhoyi are most suitable for vegetation restoration based on land cover, soil type, proximity to roads and settlements, and elevation derived from GIS and RS analysis? We hypothesize that spatial machine learning techniques can effectively model the spatiotemporal dynamics of deforestation and carbon stock changes and accurately identify optimal forest restoration sites in a rapidly urbanising landscape. This study is original in its integration of machine learning, GIS, and multi-criteria spatial analysis to examine deforestation dynamics, carbon stock losses, and restoration potential in an urbanizing African context. While previous research has largely focused on mapping land cover changes or estimating carbon stocks in isolation, our work uniquely combines RF classification of multitemporal satellite imagery with restoration prioritization using ecological, topographic, and socio-environmental criteria. This holistic framework enables the identification of areas most suitable for restoration while linking deforestation patterns to carbon emissions, providing actionable insights for sustainable urban and ecological planning. By demonstrating the applicability of this integrated approach in Chinhoyi, the study offers a replicable methodology that can inform conservation and restoration strategies in similar rapidly developing towns across Sub-Saharan Africa.

Materials and methods

Study site

Chinhoyi Town, located in Mashonaland West Province of Zimbabwe covers an area of 15,000 hectares, lies at approximately 17.35°S latitude and 30.20°E longitude (Fig. 1). It sits within the Highveld plateau at an altitude of around 1187 m above sea level. The area experiences a subtropical climate with a mean annual rainfall of about 850 mm, mostly falling between November and March [35]. Temperatures range from 7 °C in winter to over 30 °C in summer. Soils are predominantly sandy loams derived from granite, supporting moderate agricultural productivity [15]. The geology is largely underlain by the Basement Complex, characterized by granitic rocks [36]. Chinhoyi's population is growing steadily, exceeding 90,000 residents, and water availability is largely dependent on Manyame River catchment tributaries and groundwater resources. The town serves as a provincial capital and has experienced rapid urbanization and agricultural expansion in recent years, resulting in significant land use changes. Land uses in the area include residential, commercial, institutional, and agricultural activities, with maize, tobacco, and horticulture being dominant crops. Chinhoyi lies in a region that originally supported miombo woodlands, but increasing deforestation has led to severe forest cover loss, driven by urban sprawl, cultivation, firewood harvesting, and infrastructure development. The deforestation rate has intensified, with recent studies estimating forest cover reduction exceeding 50 % over the past decade [20,37].

LULC transitions and deforestation dynamics

For the purposes of LULC classification and change detection, a range of spatial datasets from multiple sources were utilized. Medium-resolution satellite imagery, specifically Landsat 7 and Landsat 8, served as the primary sources of remotely sensed data. Specifically, we define medium-resolution images as those with a spatial resolution ranging between 10 m and 100 m, following commonly accepted classifications in RS literature. This includes sensors such as Landsat (30 m) and Sentinel-2 (10–20 m). These datasets encompass various timeframes and sensor types to capture LULC transitions over time. To mitigate the influence of seasonal variability on classification outcomes, only images acquired during the same season were selected. To ensure phenological consistency, all images used were captured during the dry season—a period characterized by minimal vegetation growth variability [9].This timeframe is considered optimal for distinguishing between different LULC classes. The study employed reflective bands from Landsat imagery with a spatial resolution of 30 m to extract multi-temporal LULC change data. Raw satellite imagery must undergo pre-processing before it can be effectively used for mapping purposes [38]. Essential corrections include radiometric and geometric adjustments. Geometric distortions in raw data may arise from systematic errors, such as the relative motion between the Earth's rotation and the satellite's orbit, and from random anomalies. These distortions typically result in spatial displacement along the north-south and east-west axes. Rectification was achieved through the use of training points, aligned with georeferenced topographic

maps of the area [39]. To construct false-colour composite images, the visible, near-infrared (NIR), and shortwave infrared (SWIR) bands from Landsat 7 and 8 were layered using GEE image processing platform. The raw digital number (DN) values were then converted to spectral radiance, as recommended by Ziskin et al. [39]. Atmospheric corrections were applied to eliminate the influence of atmospheric interference, following Lillesand [40]. Thematic mapping involves categorizing spatial information to represent the geographic distribution of specific land cover types [38,40]. Satellite imagery can be systematically analysed to derive meaningful environmental information across temporal and spatial scales. The fundamental goal of classification is to assign each image pixel to a specific land cover category [41]. Several parameters influenced the selection of the classification method, including map accuracy, landscape dynamics, training data requirements, and algorithmic complexity [7]. Data analysis for LULC was carried out using Google Earth Engine (GEE) platform using the RF machine learning algorithm. The initial step involved the acquisition of Landsat Satellite imagery, followed by the creation of model training samples. Four land cover classes were created, and these included forests, built-up, bare land, and cropland. The classes were merged into a single training dataset. The second step involved the extraction of spectral information for the training data. The sampleRegions() function was used to extract spectral reflectance values from the Landsat image at the location of training samples. A mixture of natural colours and false colours was used on the Landsat imagery to properly visualise different land covers and create accurate training samples. Data from sample points was split into training and testing datasets using the randomColumn () function. To complete this task, we performed data splitting where 70 % of the data was selected for training the model, whilst the remaining 30 % was used to assess the model's accuracy. This step is crucial since an unknown dataset needs to be used to test the performance of the model. Satellite imagery for each year used in the study was classified using this method. The trained classifier was applied to the testing dataset (30 %), and its predictions were compared to the actual land cover labels. The errorMatrix() function generated a confusion matrix that was used to evaluate the model's performance. The training points extracted from the field (Fig. 1), were primarily collected for accuracy assessment of the LULC classification rather than for model training. The training samples used in the classification process were generated within the GEE platform, where stratified random sampling was conducted using visually interpreted high-resolution imagery. This approach ensured adequate spatial representation of all LULC classes while maintaining the independence of the validation dataset to avoid bias in accuracy assessment.

Change detection and deforestation identification

Analysing LULC changes is essential for informing effective land management strategies. In the context of RS, change detection involves assessing variations in the condition of a given area by utilizing spatial datasets acquired at different time intervals. The underlying principle of using satellite imagery for this purpose is that transformations in land use and cover are manifested as differences in spectral reflectance values [42]. There are three primary methods of change detection in RS: image subtraction, image ratio approach, and change detection after categorisation [43]. In this study we used the image subtraction method. Image subtraction detects changes in pixels based on their grey values. As the name suggests, the image ratio method is used to determine the ratios of pixels in each band of an image [34]. Furthermore, it is the most apparent method after independent image processing and classification for different periods [42]; hence, post-classification change detection was selected for this work. Classified images from GEE were reclassified into forest and non-forest areas. Water, bare land, built-up, and cropland were merged into a single class representing all non-forest areas, whilst forest remained an independent class. This approach was essential to simplify the visualisation and analysis of deforestation trends over time without distractions from other categories. To identify deforestation between two distinct years, reclassified images were loaded into QGIS 3.40.10, Bratislava, Slovakia (2025), and the MOLUSCE (Modules for Land Use Change Evaluation) change detection algorithm was used to perform change detection. The MOLUSCE plugin utilises cellular automata artificial neural network (CA-ANN) in analysing the transformations. The integration of RF and CA–ANN does not imply that the results are jointly dependent on both algorithms for classification. Instead, RF provided the input classified maps (historical and baseline LULC data) required by the CA–ANN model to perform spatiotemporal simulation and projection. The two models were therefore sequentially applied, each serving a specific analytical purpose—RF for accurate classification, and CA–ANN for dynamic modelling and prediction. Specifically, the classified LULC maps were first produced in GEE using the RF algorithm due to its efficient cloud-based processing and access to multi-temporal imagery. These classified outputs were then exported to QGIS for post-classification processing, including reclassification, map visualization, and conversion to the appropriate raster format compatible with the MOLUSCE plugin. Finally, MOLUSCE was used within QGIS to perform change detection and model training. Thus, the use of the classified maps across GEE, QGIS, and MOLUSCE was sequential rather than repetitive, with each platform contributing to a specific phase of the workflow. The MOLUSCE created change detection maps showing conversions from forest to non-forest areas, which represent deforestation. To calculate the area change, these maps were converted from raster to polygon due to the high accuracy of polygons in determining areas. Classified images from GEE for the two years of interest were imported into QGIS. MOLUSCE was used to detect changes from forest cover to other LULC classes between those years. This conversion was classified as deforestation, and the area coverage was calculated using the geometry tool in ArcMap 10.3 Esri (Environmental Systems Research Institute, Inc.) Redlands, California, USA, 2014. Accuracy evaluation involved both overall classification accuracy and the Kappa statistic, with the latter providing a more robust measure of agreement between classified results and reference data. In this study, Kappa values ranged between 84.35 % and 87.78 %, underscoring the algorithm's reliability in detecting LULC transitions.

Estimating above ground biomass and carbon stocks using Landsat 8 imagery

In GEE, NDVI was calculated using the Near-Infrared band (NIR) and the Red (RED) band through the formula NDVI = (NIR-RED)/(NIR+RED). AGB was then estimated using the empirical model: $a\ x$ NDVI $x\ b$, where coefficients $a = 100$ and $b = 0$. Carbon stocks

were calculated by assuming that 50 % of AGB is carbon. The equation 0.5 x AGB was used to estimate carbon stocks. Carbon stock changes were calculated by calculating the difference between 2014 carbon stocks and 2024 carbon stocks ($\Delta C = C_{14}\text{-}C_{24}$). The change in carbon stocks was masked by the deforestation layer to isolate carbon losses within deforested regions. The difference in carbon stocks was multiplied by 3.67 as the loss of 1 ton of carbon releases 3.67 tons of carbon dioxide. Histograms were generated to evaluate the distribution of AGB and carbon stocks. It should be noted that ΔC was computed only for areas of complete deforestation. While forest degradation also reduces aboveground biomass and carbon stocks, it was not included due to the limitations of our RS data in accurately detecting gradual biomass loss. Therefore, the reported ΔC represents a conservative estimate of total carbon loss.

Weighted overlay analysis for identifying areas for suitable forest restoration

Multiple spatial layers were reclassified and analysed using the GIS Weighted Overlay tool in ArcMap 10.3, to determine areas suitable for forest restoration. Factors considered in identifying potential restoration areas were roads, settlements, soil types, land use, and slope. These factors are major influencers of forest regeneration potential and ecological stability. The pairwise comparisons in Table 1 were based on expert judgment relevant literature. For instance, LULC was considered five times more important than roads due to its stronger influence on carbon sequestration and forest optimal restoration. This rationale has been added to clarify the choice of comparisons.

Weight assignment using the analytical hierarchy process (AHP)

Each factor influencing a site's potential for forest restoration was assigned a weight based on the degree of its influence in determining site suitability using the Saaty Scale [44–46]. The scale ranges from 1 and assigns weights in odd numbers, with the most significant factor assigned 1 and progressively higher values representing the least significant factors. The pairwise matrix was created to determine the comparative significance of each factor (Tables 1 and 2). Row sums from the pairwise matrix were used to compute AHP cell values (Table 3). Row sums from the AHP were summed to create a column sum, which was divided by the row sums to determine the weight of Land Use, slope, roads, settlements, and soil types in proposing the suitability of areas for forest restoration. We adapted the AHP scoring so that the most significant factor was assigned 1, with higher odd numbers for less significant factors. This is the inverse of the classic Saaty scale (1 = equal importance, 9 = extreme importance) and is clarified here to avoid confusion.

Results

LULC transitions and deforestation dynamics

The transition matrix (Table 4) denotes a shift in area coverage. The Change Matrix indicates a change in area coverage measured by hectares and the extent of change using percentage for the five periods, 2014–2016, 2016–2018, 2018–2020, 2020–2022 and 2022–2024, indicated below (Table 4). The transition matrix reveals a significant decline in the persistence of forest cover over the past 10 years, while non-forest areas demonstrated a notable increase in persistence (Table 4). By 2024, only 40.02 % of the forest cover present in 2014 remained intact, with an average persistence rate of 87.2 % calculated over two-year intervals (Table 4). This suggests the vulnerability of forest cover in Chinhoyi, emphasising the spatial and temporal dynamics in forest cover loss over time.

Deforestation dynamics

Deforestation dynamics in Chinhoyi from 2014 to 2024 reveal fluctuating trends in forest cover, deforestation rates, and forest regeneration (Fig. 2, Fig. 3, Table 5 and Table 6). Over the decade, forest cover declined from 8810 hectares in 2014 to 4001 hectares in 2024, a reduction of 54.58 %. Simultaneously, non-forest areas expanded significantly, increasing from 6225 hectares in 2014 to 11,216 hectares in 2024, representing an 80.18 % increase. Between 2014 and 2016, Chinhoyi experienced a net forest loss of 984 hectares, with 2757 hectares lost to deforestation and 1773 hectares gained through forest regeneration. From 2016 to 2018, forest cover continued to decline, with a net loss of 1381 hectares due to lower regeneration rates. The most significant forest recovery occurred from 2018 to 2020, with a net gain of 1467 hectares, attributed to a high regeneration rate of 3688 hectares. In contrast, the period from 2020 to 2022 experienced the highest deforestation, with 2962 hectares lost and a net decline of 1566 hectares. Analysis of the transition trends reveals a significant fluctuation in the 'Restored Forest' class, particularly a sharp increase during 2018–2020 followed by a drastic decline in 2020–2022 (Figure3). This pattern is not characteristic of permanent forest establishment but is highly

Table 1
Pairwise matrix.

Criteria	Land Use	Slope	Roads	Settlements	Soil Type	Row Sum
Land Use Land Cover	1	3	5	7	9	25.00
Slope	1/3	1	3	5	7	11.87
Roads	1/5	1/3	1	3	5	6.87
Settlements	1/7	1/5	1/3	1	3	4.10
Soil Type	1/9	1/7	1/5	1/3	1	2.95

Table 2
Normalised pairwise matrix.

Criteria	Land Use Land Cover	Slope	Roads	Settlements	Soil Type	Row Sum (Normalized)
Land Use Land Cover	1/25 = 0.040	3/11.87 = 0.253	5/6.87 = 0.727	7/4.10 = 0.634	9/2.95 = 0.610	2.262
Slope	1/3 ÷ 25 = 0.013	1/11.87 = 0.084	3/6.87 = 0.437	5/4.10 = 0.423	7/2.95 = 0.474	1.431
Roads	1/5 ÷ 25 = 0.080	1/3 ÷ 11.87 = 0.028	1/6.87 = 0.145	3/4.10 = 0.244	5/2.95 = 0.339	0.836
Settlements	1/7 ÷ 25= 0.057	1/5 ÷ 11.87 = 0.017	1/3 ÷ 6.87 = 0.048	1/4.10 = 0.122	3/2.95 = 0.339	0.583
Soil Type	1/9 ÷ 25 = 0.044	1/7 ÷ 11.87 = 0.012	1/5 ÷ 6.87 = 0.029	1/3 ÷ 4.10 = 0.081	1/2.95 = 0.237	0.403

Table 3
AHP table.

Factor	Most Suitable factor Score (5)	Least Suitable factor Score (1)	Weight
Land Use Land Cover	>1000 m from roads.	<100 m from roads	0.410, 41 %
Slope	0–15°	>30°	0.259, 25,9 %
Roads	>800 m from roads	<800 m from roads	0.151, 15.1 %
Settlements	>1000 m from settlements	<1000 m from settlements.	0.106, 10.06 %
Soil Type	Clay loam	Sandy	0.073, 7,3 %

Table 4
Transition probabilities of forest (F) and non-forest (NF) classes between consecutive time intervals derived from the Markov transition probability matrix (P = Probability, F = Forest; NF = Non-Forest).

Interval	P(F→F)	P(F→NF)	P(NF→F)	P(NF→NF)
2014–2016	0.524	0.313	0.188	0.921
2016–2018	1.134	0.336	0.219	1.110
2018–2020	0.538	0.342	0.579	0.987
2020–2022	0.986	0.455	0.127	1.347
2022–2024	1.177	0.245	0.287	0.996

indicative of seasonal or cyclical land cover change. We interpret this signal as likely representing temporary vegetation regrowth on fallow agricultural land or the seasonal greening and browning of grasslands within the savanna ecosystem. The significant 'loss' of this class in the 2020–2022 period likely corresponds to these areas being recleared for cultivation, affected by drought, or burned. Consequently, our use of the term 'Restored Forest' primarily applies to the more stable net gain observed over the entire decade (2014–2024), while shorter-interval changes reflect these dynamic, non-permanent land use processes. From 2022 to 2024, forest regeneration rebounded, with a net gain of 1553 hectares, marking the lowest deforestation during the study period (Fig. 4). Non-forest cover showed an overall remarkable persistence of 94.97 % with an average persistence of 107.2 % over two-year intervals. This indicates that once forest cover is lost, the likelihood of these areas reverting to forest is low. In fact, only 6.61 % of non-forest cover transitioned to forest over the 10 years (Table 6).

Table 7 illustrates the loss of forest cover due to encroachment from built-up areas and cropland in Chinhoyi over five consecutive two-year periods between 2014 and 2024. The data shows bare land as the major driver behind forest cover loss in Chinhoyi throughout the 10-year period. The highest conversion of forest to bare land occurred between 2020 and 2022, totalling 2274 hectares. On the contrary, conversions from forest cover to cropland reduced significantly from 915 hectares between 2014 and 2016 to only 173 hectares in 2024. This suggests a decline in the contribution of cropland to forest cover losses in Chinhoyi. Forest cover loss from built-up increased from 126 hectares in 2014 to a peak of 448 hectares between 2022 and 2024, which suggests intensified infrastructural development during this time. However, this trend was reversed between 2022 and 2024, with a decline in forest losses from built-up of 211 hectares. Fig. 4 gives a clear visualisation of variations in forest cover losses from different LULC.

Carbon stock change and estimation of carbon emissions from deforestation

Fig. 5 presents a comparative illustration of carbon stocks in Chinhoyi for 2014 and 2024. The data indicates a significant decline of 76,131 tonnes in carbon stocks, decreasing from 201,682 tonnes in 2014 to 125,551 tonnes in 2024. This represents a 37.73 % reduction in carbon stocks over a decade. Deforestation played a crucial role in this loss, with 12,338 tonnes of the total carbon losses attributed to it (Fig. 6 and Table 8). This deforestation resulted in the emission of 45,252.33 tonnes of carbon dioxide.

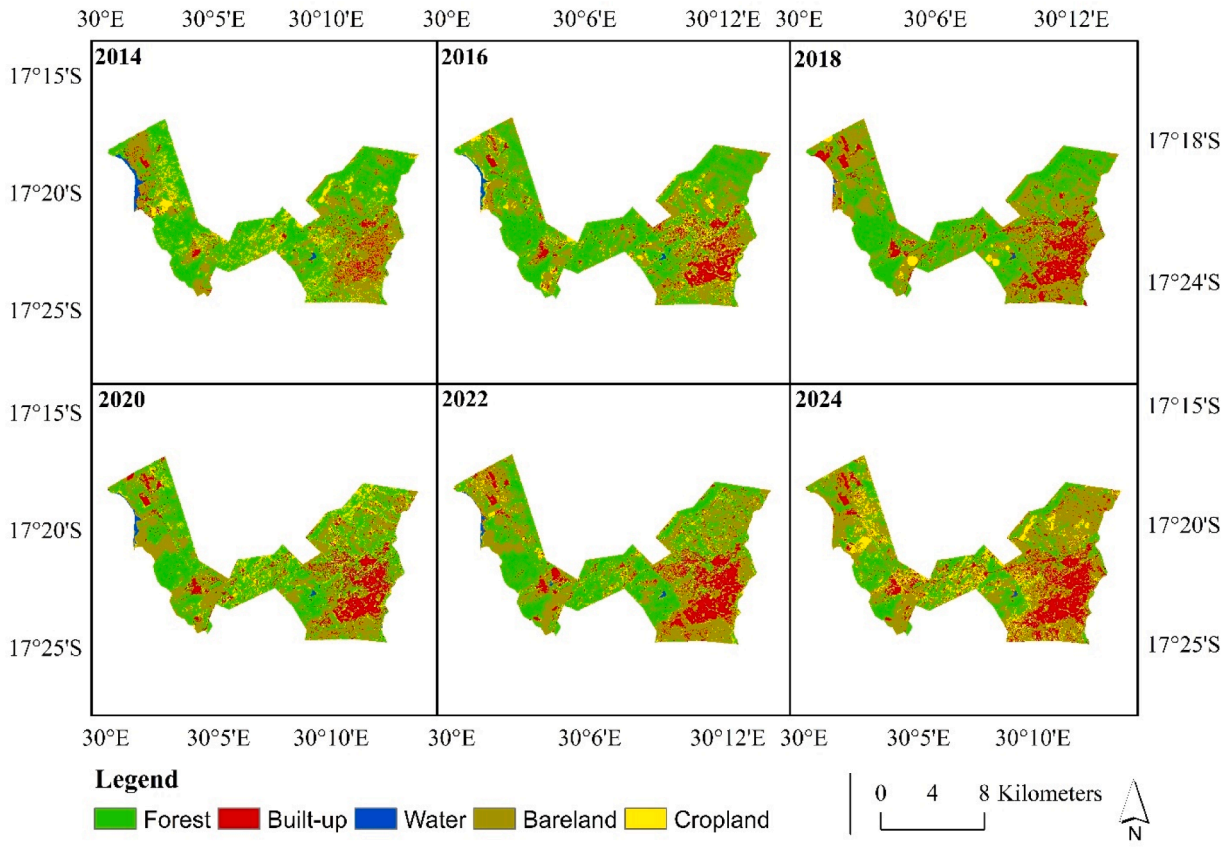

Fig. 2. Land use and land cover (LULC) maps of Chinhoyi, Zimbabwe, for the years 2014, 2016, 2018, 2020, 2022, and 2024. Forest, built-up areas, water bodies, bareland, and cropland are represented by green, red, blue, brown, and yellow colours, respectively. The maps show spatial changes in LULC over the 2014–2024 period.

Identification of suitable areas for forest restoration using overlay analysis

The site suitability analysis reveals a diverse distribution of potential restoration sites in Chinhoyi (Fig. 7). These sites are divided into five categories, and their area coverage is measured in hectares. Areas of moderate suitability cover 6633 hectares, which is the largest compared to other categories (Table 9). These areas have a moderate potential for successful forest restoration. An additional 3644 hectares fall under areas suitable for restoration. These areas have favourable conditions for successful restoration. A much smaller but highly promising 815 hectares is classified as a highly suitable area. These areas have the highest restoration potential, and they can be prioritised as targets for first interventions. On the other hand, 2514 hectares were less suitable, and an additional 1293 hectares were not suitable for forest restoration. In total, 11,092 hectares in Chinhoyi are suitable for forest restoration, and these areas include moderately suitable, suitable, and highly suitable categories.

Appendix 1 depicts the spatial distribution of distances from settlements in Chinhoyi (Appendix 1), with values ranging from 0 m to a maximum of 3852 m. Areas close to settlements, indicated in red, are predominantly concentrated in the central and southern parts of the study area. These regions represent zones of immediate proximity to human activities, including agricultural, residential, and possibly industrial areas. In contrast, areas farther away from settlements, represented by green shades, are mostly located towards the northern and north-eastern boundaries of the study area. These regions are likely to experience less human disturbance and could serve as critical zones for ecological conservation or natural habitats. The gradient from red to green demonstrates a clear spatial transition influenced by the distribution of settlements. This spatial analysis provides crucial insights into land use planning, especially regarding the relationship between settlement patterns and accessibility to services or resources.

The distribution of distances from road networks in Chinhoyi is depicted in Appendix 2. Areas that are intermediate to roads are shown in green and include those that lie between 0 and 500 m. These areas are densely concentrated in the central part of Chinhoyi, as it contains human settlements, industrial areas, and the CBD, thus necessitating accessibility. Areas furthest from human settlements are represented in white and cover distances from 1500 to 2672 m from roads, occupying the outer fringes of Chinhoyi. These areas consist of more isolated or sparsely connected settlements that lack direct road access. As a result of their remoteness, these areas have less human activity and pressure, which reduces their risk of logging, agricultural expansion, and infrastructural development. The distinct green-to-white gradient, therefore, highlights how Chinhoyi's road accessibility affects the suitability of regions for forest

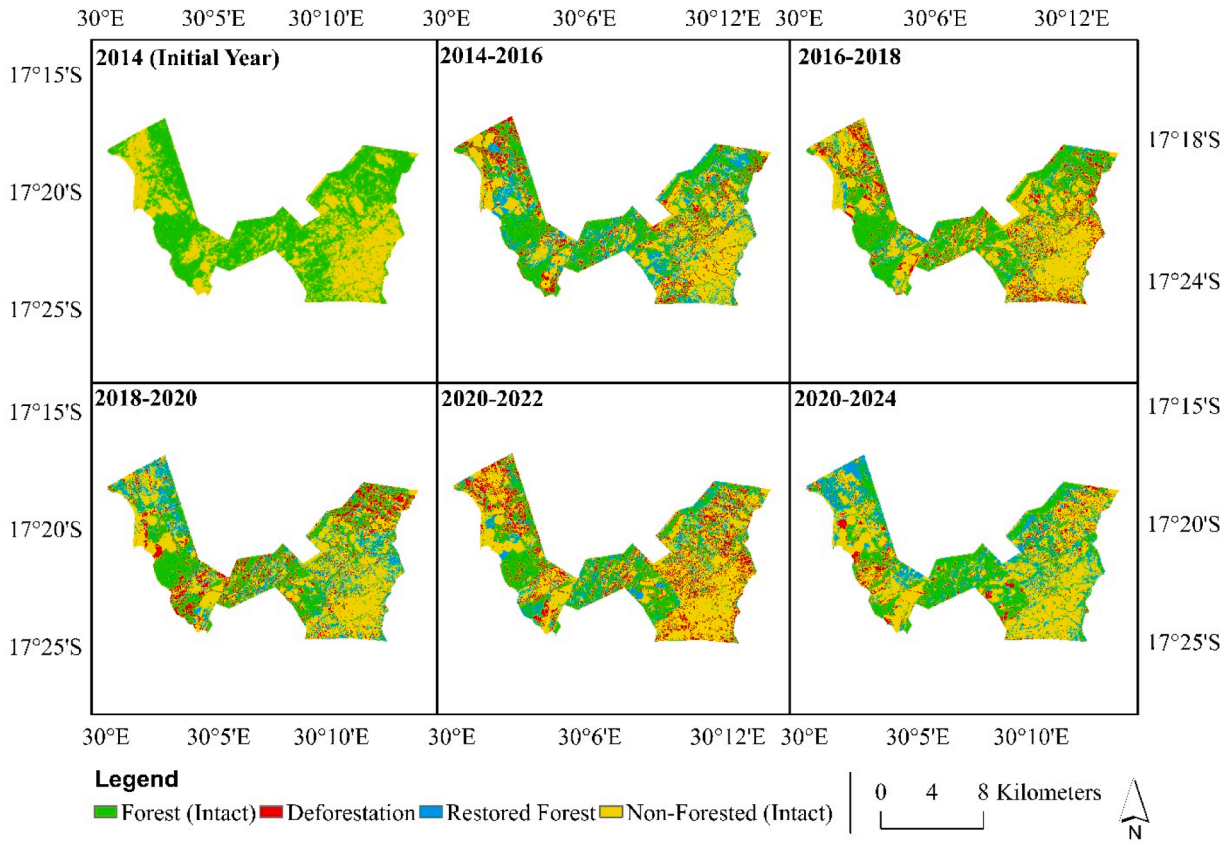

Fig. 3. Time series change maps illustrating trends in deforestation, restoration, forest, and non-forest (2014–2024).

Table 5
LULC change dynamics in Chinhoyi between 2014 and 2024, showing the area (in hectares) of forest, deforested, restored forest, and non-forest classes for each time interval (Values represent area in hectares; Forest (Intact) = areas remaining forested; Deforestation = areas converted from forest to non-forest; Restored Forest = areas converted from non-forest back to forest; Non-Forest (Intact) = areas remaining non-forest).

Year	2014	2014–2016	2016–2018	2018–2020	2020–2022	2022–2024	2014–2024
Forest (Intact)	8810	4623	5242	2819	2780	3271	3526
Deforestation		2757	2151	2221	2962	877	5304
Restored Forest		1773	1254	3688	804	2430	412
Non-Forest (Intact)	6225	5732	6368	6287	8469	8437	5912

Table 6
Land Cover Transition Matrix for Chinhoyi (2014–2024). Values represent the percentage of the total landscape or the percentage of the initial class that transitioned to another class by 2024. ("Forest" class corresponds to "Restored Forest" areas. The "Non-Forest" class includes areas identified as "Deforestation" as well as other persistent non-forest land cover types).

	Forest	Non-Forest
Forest	40.02 %	60.20 %
Non-Forest	6.61 %	94.97 %

restoration, with suitability increasing as accessibility decreases.

The slope of Chinhoyi ranges from 0° to 36.63°, with some areas featuring flat terrain while others comprise steep hills (Appendix 3). The regions that are flat are represented by brown and yellow shades, making them more likely to have deeper, moist, and fertile soils suitable for restoration. In contrast, the areas represented by green and blue shades are steep, dry hills that possess shallow soils and are prone to erosion. This variation in slope significantly influences the suitability for restoration efforts, with gentler

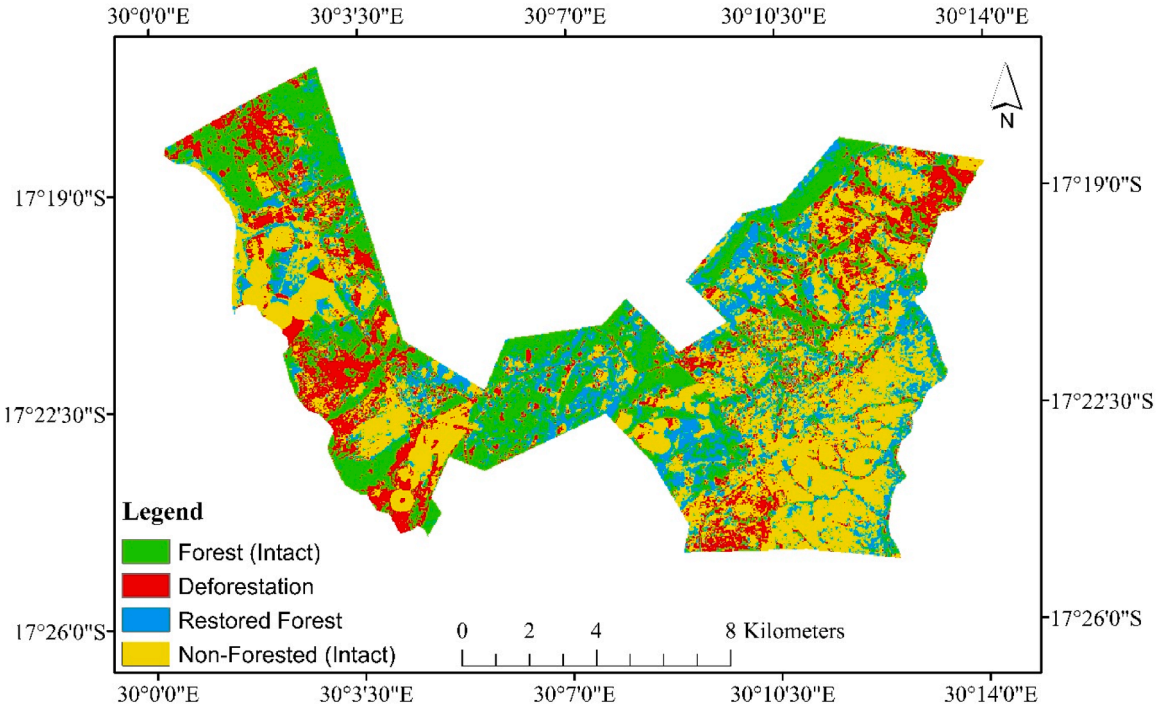

Fig. 4. Overall LULC map of Chinhoyi, Zimbabwe, for the years 2014–2024. The map depict the spatial distribution and transitions between intact forest, deforestation, restored forest, and non-forested areas over the study period.

Table 7
Forest cover conversions to bare land, cropland, and built-up in Chinhoyi (2014 to 2024).

Period	Forest-Built-up (hectares)	Forest to Bare-land (hectares)	Forest to Cropland (hectares)
2014–2016	126	1716	915
2016–2018	142	1547	460
2018–2020	301	1463	449
2020–2022	448	2274	231
2022–2024	211	487	173

slopes being more favourable than steeper ones.

Discussion

LULC transitions and deforestation dynamics

The application of RF machine learning, integrated with GIS and multitemporal satellite imagery, has provided a powerful and statistically robust approach to detect and model deforestation dynamics in Chinhoyi from 2014 to 2024. Through a synergistic integration of remotely sensed data and spatial analysis, this study has contributed not only to identifying land cover transitions but also to interpreting the underlying spatiotemporal patterns and drivers of deforestation. Such methodological rigor is instrumental in understanding ecosystem dynamics and informing targeted conservation and restoration efforts, particularly in rapidly urbanizing landscapes. RF, a supervised ensemble learning algorithm, is well-suited for land cover classification tasks due to its non-parametric nature, high classification accuracy, and ability to handle complex, non-linear relationships between predictor variables [47,48]. In this study, RF was applied to Landsat 7 and 8 imagery to classify LULC into forest and non-forest categories six times across a decade. The integration of RF with GIS facilitated spatially explicit classifications and subsequent temporal comparisons, allowing the generation of accurate LULC maps with user and producer accuracies exceeding 84 %, and Kappa coefficients above 0.82. These metrics confirm the statistical robustness of the classification and ensure reliable insights into the temporal progression of deforestation. The multitemporal nature of satellite imagery allowed for comprehensive tracking of land cover changes at two-year intervals. This fine temporal resolution revealed the episodic and uneven nature of deforestation across the decade, with significant gains and losses in forest cover reflecting both anthropogenic pressures and periods of regeneration [49]. GIS tools were essential in visualizing, quantifying, and analysing these changes, enabling the construction of change matrices, transition probabilities, and spatial overlays that

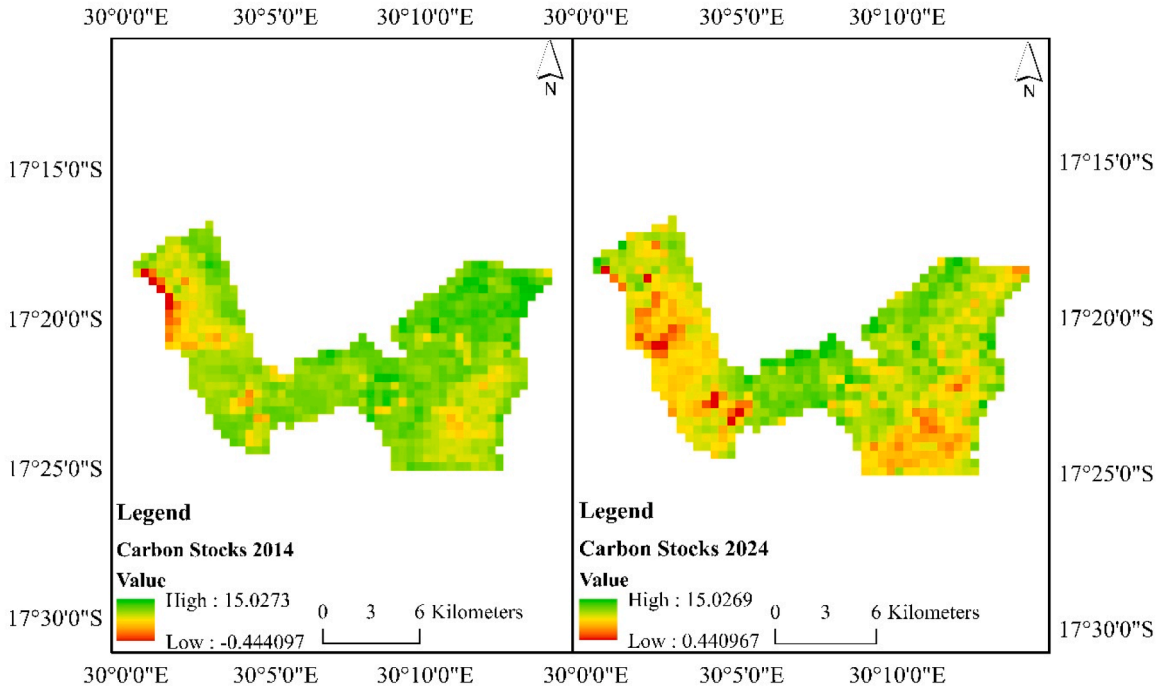

Fig. 5. A Comparison Map between Carbon Stocks (tonnes/hectares) in 2014 and Carbon Stocks in 2024.

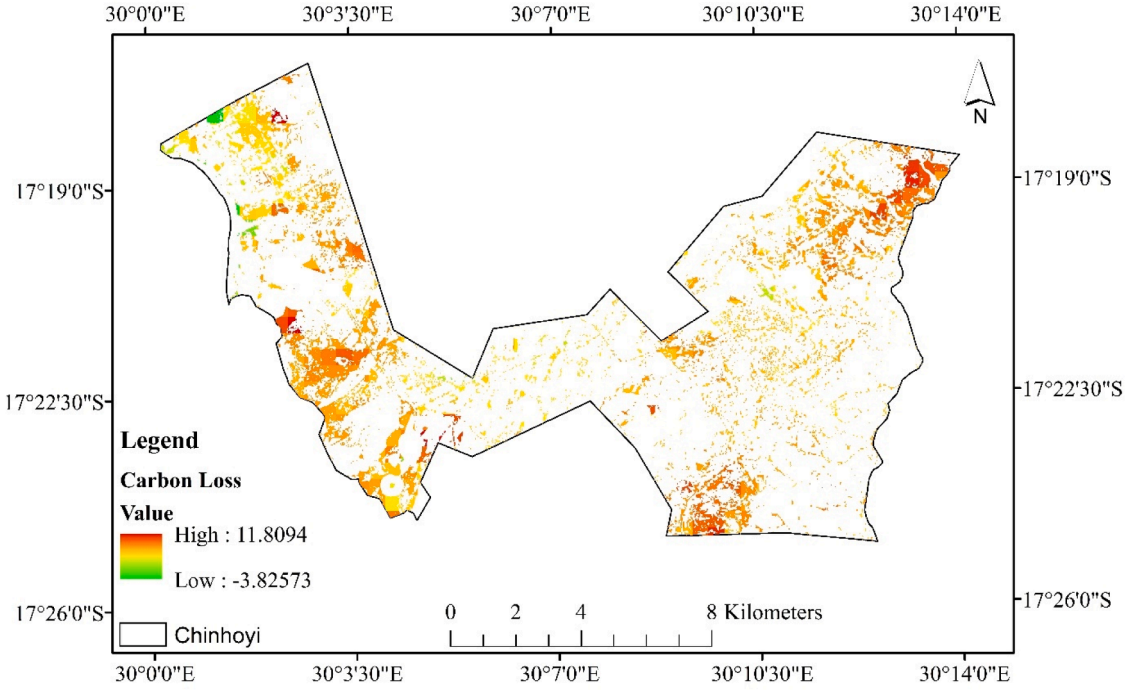

Fig. 6. Distribution of carbon gains and losses (tonnes/hectares) in Deforested areas of Chinhoyi (2014–2024).

reveal where, when, and how land cover transformation occurred [50]. By calculating transition probabilities (e.g., P(F→NF) and P (NF→F)), the study captured the likelihood of forest loss and gain across different intervals. These figures reveal both the persistence and vulnerability of forested landscapes under urban pressure. For instance, the relatively low probability of non-forest transitioning back to forest (6.61 % over the decade) underscores the difficulty of achieving spontaneous regeneration in disturbed environments,

Table 8
Net change in carbon stocks resulting from land cover transitions in Chinhoyi (2014–2024).

Carbon Stocks (tonnes/hectares)	Area(hectares)	Carbon Gain and Losses	Total carbon stocks (tonnes)
−4	0	Gain	0
−3	15	Gain	45
−2	1	Gain	2
−1	9	Gain	9
1	25	Loss	25
2	36	Loss	72
3	291	Loss	873
4	498	Loss	1992
5	761	Loss	3805
6	510	Loss	3060
7	195	Loss	1365
8	120	Loss	960
9	16	Loss	144
10	3	Loss	30
12	1	Loss	12
	Total		12,338

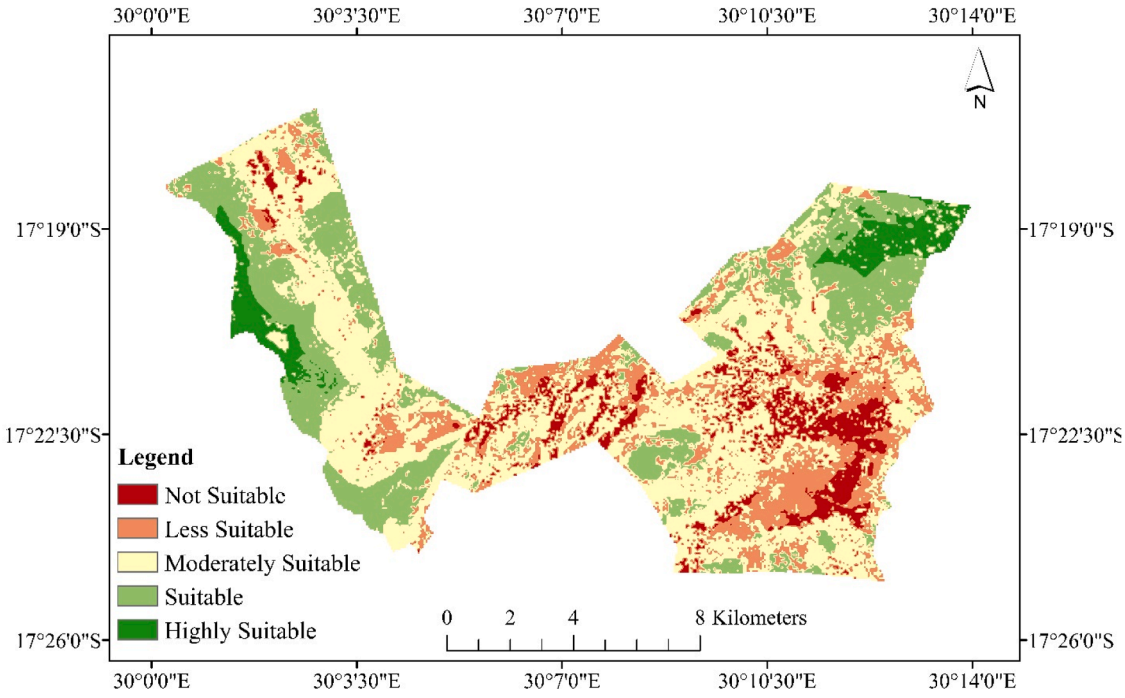

Fig. 7. Spatial suitability map for forest landscape restoration in Chinhoyi, Zimbabwe. The map identifies areas with high potential for successful restoration interventions based on LULC data.

Table 9
Area suitability in hectares.

Suitability category	Area (Hectares)
Not Suitable	1293
Less Suitable	2514
Moderately Suitable	6633
Suitable	3644
Highly Suitable	815

while the higher persistence of non-forest areas (94.97 %) confirms the dominance of irreversible land cover conversions once forests are cleared.

The spatial and temporal dynamics observed in Chinhoyi reflect broader urbanization and land transformation trends seen in many African secondary cities. Forest loss in the town was closely associated with three key drivers: expansion of bare land, growth of built-

up areas, and agricultural encroachment. Of these, conversion to bare land emerged as the dominant factor, with a peak transformation of 2274 hectares occurring between 2020 and 2022. This trend signals the emergence of fallow or degraded lands, possibly due to informal settlements, sand mining, or deforestation without immediate land reuse, indicating unsustainable land use practices. Built-up expansion contributed significantly to forest loss, peaking at 448 hectares between 2020 and 2022, suggesting increased infrastructure development during this period. While this declined in the subsequent period, it still indicates a clear trend of urban sprawl [36]. Interestingly, forest-to-cropland conversions decreased over time, suggesting a possible saturation of cultivable land within town boundaries or a shift in land-use priorities. The combination of satellite data, classification accuracy metrics, and transition matrices enables these nuanced interpretations of landscape change. The calculated forest persistence rate of only 40.02 % from 2014 to 2024 reveals the fragility of the region's forest ecosystems. When overlaid with spatial maps, these dynamics present critical hotspots of deforestation, areas of active regeneration, and zones at risk of further degradation. This form of spatial modeling provides the basis for identifying optimal forest restoration sites [1], one of the major objectives of this study. Such insights are invaluable for urban planners, conservationists, and policymakers seeking to mitigate deforestation and plan effective restoration strategies.

The methodology and findings of this study are transferable and highly relevant to many urbanizing areas across sub-Saharan Africa. Rapid urban expansion is a defining feature of African towns and cities, often occurring in the absence of structured land use planning. The Chinhoyi case demonstrates how combining RF, GIS, and satellite imagery can produce actionable intelligence to guide urban ecological sustainability. Cities like Kisumu in Kenya, Bamenda in Cameroon or Gulu in Uganda are undergoing similar pressures, with forests on their peripheries being cleared for settlements, agriculture, or infrastructure [51–53]. Applying this framework in such contexts would enable the mapping of land cover trajectories, detection of critical ecosystem loss areas, and formulation of targeted restoration interventions. Moreover, this approach can support land degradation neutrality (LDN) initiatives under the United Nations Convention to Combat Desertification (UNCCD) framework, Reducing Emissions from Deforestation and Forest Degradation (REDD+), and national reforestation and climate resilience strategies [54]. Another key application lies in informing urban green infrastructure planning. By identifying where forest loss has occurred and where restoration potential remains high (e.g., areas where regeneration has previously occurred), decision-makers can spatially prioritize reforestation, agroforestry, or urban park development. While it is true that the restoration area is located away from urban centers, the mention of urban park development is intended as a potential future application or conceptual option rather than a current implementation. The area's ecological restoration creates opportunities for recreational, educational, and ecotourism functions that could eventually be linked with nearby settlements through green corridors or planned infrastructure. This approach aligns with global strategies where restored landscapes, even in peri-urban or remote areas, can serve as satellite urban parks or nature-based recreational zones, contributing to biodiversity conservation and community engagement. Additionally, modeling land cover change using RF can assist in scenario-based planning, allowing stakeholders to visualize how future expansion might affect ecological assets under different land-use policies. From a scientific perspective, the integration of temporal change analysis with machine learning classification contributes to improving methodologies for land change science. The temporal disaggregation employed in this study (two-year intervals) offers more detailed insights than traditional five- or ten-year assessments, making it easier to capture event-driven land change processes, such as those linked to policy shifts, climatic shocks, or economic changes.

Carbon stock change and estimation of carbon emissions from deforestation

The estimation of carbon stock losses and associated carbon dioxide (CO_2) emissions from deforestation in Chinhoyi between 2014 and 2024 offers a critical lens through which the ecological consequences of land use change can be quantified. Utilizing AGB estimation methods in conjunction with spatial machine learning techniques, this study captures the magnitude of ecosystem degradation in both biophysical and atmospheric terms. The application of this methodological framework holds significant implications for climate change mitigation, sustainable land management, and carbon accounting in Africa's rapidly transforming landscapes.

Between 2014 and 2024, Chinhoyi experienced a net reduction of 76,131 tons in carbon stocks, primarily driven by widespread forest clearing and land conversion. Of this decline, 12,338 tons were directly attributable to deforestation events, corresponding to an emission of approximately 45,252.33 tons of CO_2 into the atmosphere. These estimates were derived using standardized AGB biomass-to-carbon conversion approaches. The biomass values were estimated per hectare, then multiplied by the area of deforestation for each biomass class, before applying a carbon fraction (usually 0.5) and converting the carbon stock into CO_2 equivalents using a multiplier of 3.67 (based on molecular weights of carbon and CO_2). This method provides a scientifically rigorous, spatially explicit accounting of how deforestation contributes to greenhouse gas (GHG) emissions, thus bridging RS, ecology, and atmospheric science [3].

AGB estimation relies heavily on accurate LULC classification, vegetation indices, canopy structure data, and field validation [50]. In this study, spatial machine learning — specifically the RF algorithm — enabled highly accurate classification of forested and non-forested areas. This classification, in turn, formed the foundation for allocating ABG values to different land cover types based on pre-defined biomass classes [55]. By using multi-temporal satellite imagery from Landsat and integrating the output into a GIS framework, biomass loss could be spatially mapped, quantified, and linked to specific areas of forest degradation [56,57]. The significance of applying AGB estimation lies in its capacity to incorporate both above-ground biomass (tree trunks, branches, leaves) and below-ground biomass (roots), providing a more holistic assessment of carbon storage. Many traditional methods overlook below-ground biomass due to data limitations, yet it accounts for up to 20–30 % of total biomass in many forest systems. Hence, the use

of a comprehensive AGB approach in this study allows for more precise carbon accounting and highlights the true ecological cost of forest loss.

The results demonstrate that urban-driven deforestation in small but rapidly growing towns such as Chinhoyi can contribute significantly to atmospheric carbon concentrations. Emissions of over 45,000 tons of CO_2 from deforestation alone underscore the hidden climate costs of land development and infrastructure expansion. This is especially concerning in regions that do not yet have formal emissions reporting mechanisms or integrated urban sustainability plans. These carbon losses not only undermine Zimbabwe's commitments under the Paris Agreement and its Nationally Determined Contributions (NDCs), but also erode the ecological resilience of local landscapes [26]. Forests serve as carbon sinks, biodiversity reservoirs, and climate regulators — and their degradation diminishes the ability of ecosystems to adapt to climate extremes such as droughts, floods, and heatwaves. As such, this study provides critical baseline data for designing climate-smart urban policies, including green infrastructure, forest conservation, and ecosystem restoration strategies.

While this study focused on Chinhoyi, the methodological framework is transferable to many other African regions experiencing deforestation. Countries such as Nigeria, Ghana, Uganda, and the Democratic Republic of Congo face similar challenges as rural landscapes are converted into urban and peri-urban zones, often without adequate land-use planning. By integrating ABG estimation with geospatial machine learning, national governments, conservation agencies, and urban planners can: (i) quantify national and sub-national carbon emissions from deforestation with high spatial resolution (ii) identify carbon-rich hotspots for targeted protection or reforestation (iii) monitor the effectiveness of forest restoration efforts over time using satellite-based biomass change detection and (iv) develop incentive-based carbon offset programs (e.g., REDD+), where verified emissions reductions can be monetized. Moreover, this approach complements Africa's increasing push toward the Digital Earth paradigm [58,59] — using geospatial data to inform environmental governance. By leveraging freely available RS data, open-source algorithms, and ABG carbon models, the continent can scale up spatial carbon accounting at relatively low cost. This is particularly important given Africa's low historic emissions but high vulnerability to climate change impacts.

The transition from forested to urbanized land, as seen in Chinhoyi, reflects a broader developmental trajectory common across many African cities. However, this transformation need not come at the expense of environmental integrity. Spatial carbon analysis, as demonstrated here, offers an evidence-based platform to balance growth and sustainability. For example, zoning regulations can incorporate carbon stock data to avoid high-biomass areas, while urban green belts can be established in degraded zones with high restoration potential [24]. Furthermore, integrating carbon accounting into Environmental Impact Assessments (EIAs) could become a standard practice for future developments [11]. To facilitate such transitions, capacity building in geospatial technology and carbon modeling is essential. Universities, government agencies, and regional research institutions must invest in training programs that equip stakeholders with the skills to perform ABG-based carbon assessments and interpret satellite data effectively.

Identification of suitable areas for forest restoration using overlay analysis

The identification of suitable areas for forest restoration using multi-criteria suitability analysis in Chinhoyi presents a compelling case for the strategic integration of GIS, RS, and spatial decision support tools in environmental planning. By combining ecological, infrastructural, and socio-environmental datasets—specifically land cover, soil type, proximity to roads and settlements, and elevation/slope—this study adopts a holistic landscape-based approach to determine restoration potential.

The methodology adopted in this study builds on the strength of overlay-based spatial modelling, where each biophysical and anthropogenic criterion is assigned a weight based on its relative importance to forest regeneration potential. The AHP method, pioneered by Saaty [44], is applied to objectively derive these weights through pairwise comparisons, ensuring that expert judgment is systematically and mathematically incorporated into the spatial decision-making process. This ensures that more influential variables (e.g., slope or proximity to human activity) have a stronger impact on the suitability classification, while less critical factors are proportionately down-weighted. The Weighted Overlay Analysis synthesizes these inputs in GIS to generate a composite suitability map, categorizing the landscape into five classes: highly suitable, suitable, moderately suitable, less suitable, and not suitable. The outcome is a spatially explicit, decision-ready map that highlights zones where restoration would yield the highest ecological returns with the least socio-environmental conflict. Importantly, this approach acknowledges that land suitability for restoration is gradient-based, not binary, and that multiple environmental constraints must be considered simultaneously.

The spatial configuration of suitable areas in Chinhoyi reflects complex interactions between natural topography and human land use. For example, areas closer to settlements and roads are more accessible for restoration efforts but may suffer from increased anthropogenic disturbance, land competition, or land tenure complexities. Conversely, remote areas with low accessibility—while offering reduced human pressure—may face challenges related to monitoring, enforcement, and logistical feasibility. Therefore, the inclusion of both proximity-to-roads and proximity-to-settlements criteria helps to balance ecological suitability with practical implementation considerations [5]. Similarly, slope and elevation significantly influence restoration potential. Flat and gently sloping areas—often characterized by deeper, moisture-retentive soils—are more conducive to tree establishment and long-term forest stability [2]. In contrast, steep slopes are more prone to erosion, shallow rooting zones, and runoff, which can hinder reforestation success. Thus, assigning higher suitability scores to flatter terrains aligns with ecological restoration principles and ensures greater likelihood of achieving vegetation permanence. The final suitability map revealed that over 11,000 hectares in Chinhoyi are viable for

forest restoration, with areas categorized as highly suitable offering immediate opportunities for conservation action. These zones represent the intersection of ecological viability and minimal land use conflict, and they should be prioritized for pilot reforestation projects, biodiversity corridors, or community woodlots. Areas of moderate and suitable classification, while not optimal, still offer restoration opportunities under managed scenarios or with added investments such as soil amendment, fencing, or community engagement.

We emphasize that the workflow presented here was developed and tested only for the Chinhoyi study area and therefore its external validity remains to be demonstrated. The approach is intentionally modular — combining a RF classifier applied to multi-temporal satellite imagery with GIS-based spatial analyses and AGB→C conversions — and thus can be adapted for use in other regions that have comparable remote-sensing and ancillary data. However, transfer to other locations requires local calibration and explicit validation. Specifically, users must (i) obtain representative local training samples or use transfer-learning approaches, (ii) harmonize sensor/scene characteristics and pre-processing steps across sites, (iii) select or derive appropriate local allometric equations and carbon-fraction values for biomass→carbon conversions, and (iv) perform independent accuracy assessment (including cross-site validation where possible) and uncertainty/sensitivity analysis. Until such external applications and cross-region tests are performed, we limit our conclusions to the method's demonstrated performance in Chinhoyi and recommend that future studies validate the workflow at one or more contrasting sites to quantify its generalizability.

To contextualize our results, we compared local forest change estimates with international datasets, including the Global Forest Change dataset (v1.12) and the annual global forest gain dataset by Du et al. [20]. Our findings show general agreement with these global datasets, providing a benchmark that reinforces the reliability of the locally derived Landsat-based Forest loss and gain estimates, while highlighting some local-scale variations [20].

The results of this study highlight the importance of proactive spatial planning in forest restoration. By identifying restoration-priority areas in advance, local governments and environmental agencies can integrate these zones into urban development plans, conservation strategies, and disaster risk reduction frameworks. For example, highly suitable areas can be earmarked as part of green infrastructure networks, while moderately suitable areas can be targeted for agroforestry systems or reforestation with community participation. Moreover, the spatial data produced can support evidence-based funding applications to international climate and biodiversity finance mechanisms, such as the Green Climate Fund, the Global Environment Facility, or African Forest Landscape Restoration Initiative (AFR100). These platforms require clear, spatially grounded justifications for proposed restoration actions—exactly the kind of insight provided by multi-criteria GIS analysis. To ensure sustainability, local stakeholder engagement must accompany any implementation phase. The suitability of a site for restoration is not only biophysically determined but also socially constructed. Understanding land tenure systems, cultural values, and community preferences is essential in translating mapped potential into tangible restoration outcomes.

Our suitability analysis identified extensive areas of bare land as 'highly suitable' for restoration. This finding, while potentially counterintuitive, is grounded in practical restoration ecology. Firstly, bare lands often represent areas of prior degradation (e.g., from overgrazing, failed cultivation, or erosion) but have not undergone a complete loss of soil seed banks or soil fertility. Their very status as 'bare' signifies a critical need for intervention to prevent further land degradation and desertification. Restoring these areas directly tackles the source of degradation and can yield significant ecological dividends. The potential positive influences on soil and climatic conditions are substantial. Restoration of bare land through the establishment of native trees and grasses can (i) improve soil health: Plant roots bind the soil, reducing erosion. Leaf litter and organic matter from vegetation replenish soil nutrients, enhance soil organic carbon, and improve water infiltration and retention capacity, combating the hardpan conditions typical of degraded bare lands (ii) modify micro-climatic conditions: The introduction of vegetation provides shade, lowers soil surface temperatures, and increases evapotranspiration, leading to a more humid and stable local microclimate. This is crucial in semi-arid regions like Chinhoyi. (iii) cost-effectiveness and social feasibility: From a socio-economic perspective, targeting bare lands often faces fewer conflicts than converting active agricultural land or even modifying existing forests. It represents a 'win-win' scenario, restoring ecosystem services without directly displacing current productive land uses. In contrast, while our model also indicated suitability within some forested areas, these are likely candidates for assisted natural regeneration or enrichment planting, rather than full-scale restoration. The goal in these areas is to improve the density and quality of existing forests, not to convert them. Therefore, the prioritization of bare lands is strategically sound, as it focuses efforts on areas where the potential for net ecosystem gain is greatest and the opportunity cost is lowest, thereby aligning with the principles of FLR.

Conclusion

This study investigated deforestation dynamics, carbon stock loss, and restoration suitability in Chinhoyi, Zimbabwe, using integrated RS, GIS, and machine learning approaches. First, the spatial and temporal analysis revealed a pronounced decline in forest cover between 2014 and 2024, largely driven by agricultural expansion, urbanisation, and land degradation, with only localized and intermittent regeneration observed. These patterns indicate a landscape undergoing sustained net forest loss despite minor recovery processes. Second, deforestation over the study period resulted in substantial carbon stock depletion and corresponding carbon dioxide emissions, confirming the significant contribution of land cover change to carbon fluxes and reinforcing the role of forests in climate regulation within rapidly urbanising regions. Third, the suitability analysis identified priority areas for vegetation restoration,

primarily characterised by favourable land cover, soil conditions, moderate slopes, and accessibility to roads and settlements, providing a spatially explicit basis for targeted intervention. Overall, the study highlights the effectiveness of integrating machine learning with geospatial analysis for environmental monitoring and decision-making. However, limitations related to medium-resolution imagery and exclusion of forest degradation suggest that carbon loss estimates may be conservative, warranting further research using higher-resolution data and field validation.

Author contributions

Nobert Tafadzwa Mukomberanwa: Conceptualization, Formal analysis, Methodology, Software, Supervision, Validation, Visualization, Writing – original draft, Writing – review & editing.

Talent Kamanga: Conceptualization, Data curation, Formal analysis, Methodology, Software, Visualization, Writing – original draft, Writing – review & editing.

Blessing Onias Munetsi: Conceptualization, Formal analysis, Methodology Writing – review & editing.

Funding

There was no funding associated with this study.

Data availability

The data that support the findings of this study are available on request from the corresponding author.

Declaration of competing interest

The authors declare no conflict of interest associated with this paper.

Acknowledgements

The authors would want to acknowledge the role of anonymous reviewers who helped to enhance the quality of the work.

Appendix 1. Distances from settlements

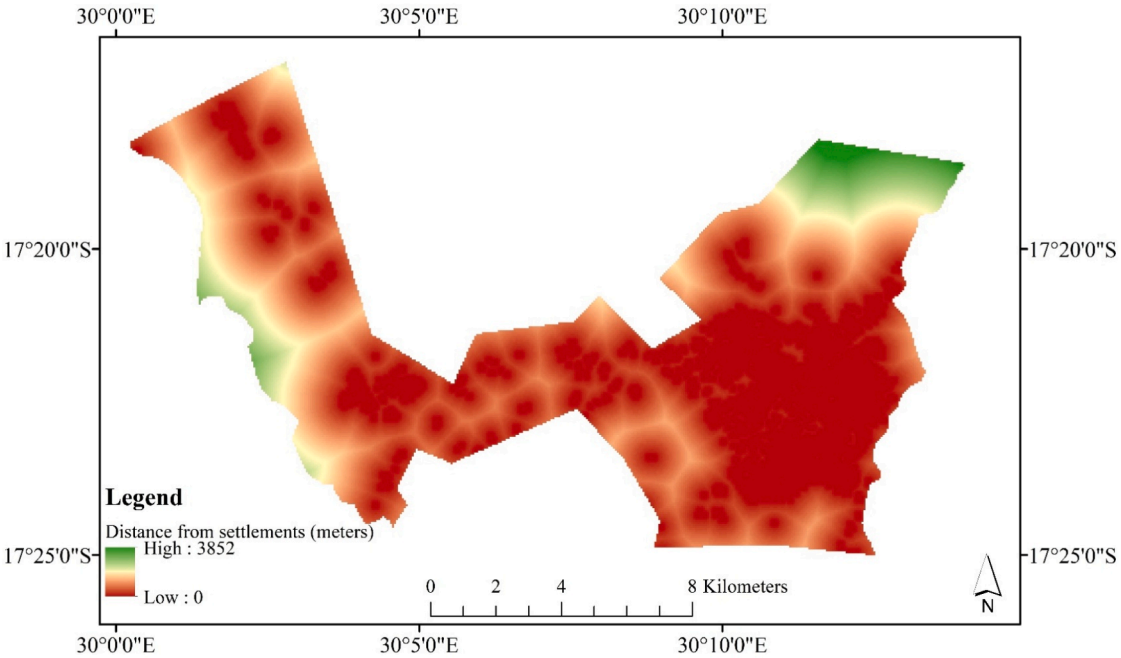

Appendix 2. Distance from roads

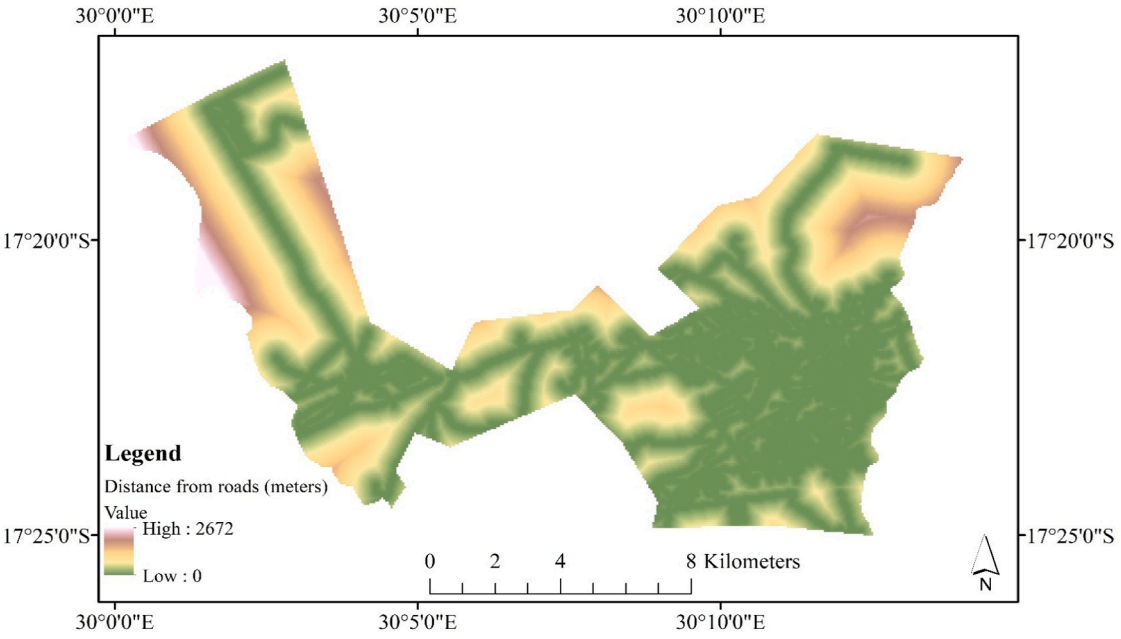

Appendix 3. Slope Variations across Chinhoyi

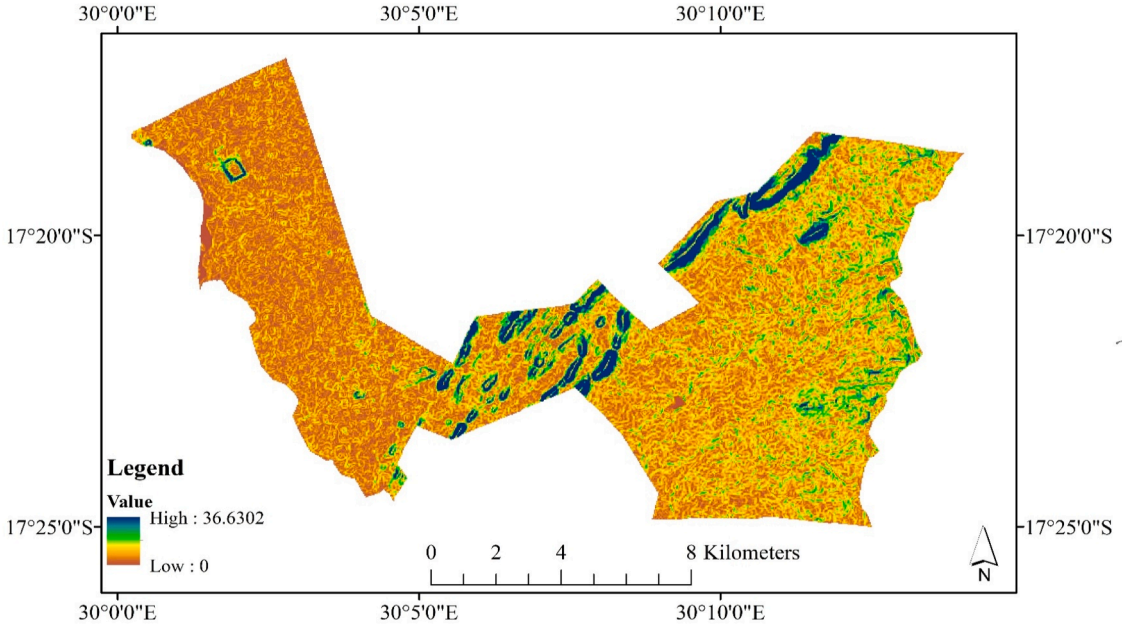

References

[1] R.A. Viani, T.E. Barreto, F.T. Farah, R.R. Rodrigues, P.H. Brancalion, Monitoring young tropical forest restoration sites: how much to measure? Trop Conserv. Sci. 11 (2018), 1940082918780916.
[2] T.K. Thakur, S. Swamy, A. Thakur, A. Mishra, S. Bakshi, A. Kumar, M.M. Altaf, R. Kumar, Land cover changes and carbon dynamics in Central India's dry tropical forests: a 25-year assessment and nature-based eco-restoration approaches, J. Environ. Manage 351 (2024) 119809.
[3] Z. Zhang, Z. Wang, X. Zhang, S. Yang, Estimation of spatial–Temporal dynamic evolution of potential afforestation land and its carbon sequestration capacity in China, Remote Sens. (Basel) 16 (16) (2024) 3098.
[4] F. Orsi, D. Geneletti, A.C. Newton, Towards a common set of criteria and indicators to identify forest restoration priorities: an expert panel-based approach, Ecol. Indic. 11 (2) (2011) 337–347.
[5] S. Li, Y. Cao, J. Liu, S. Wang, W. Zhou, Assessing spatiotemporal dynamics of land use and cover change and carbon storage in China's ecological conservation pilot zone: a case study in Fujian Province, Remote Sens. (Basel) 14 (16) (2022) 4111.
[6] X. Chang, Y. Xing, J. Wang, H. Yang, W. Gong, Effects of land use and cover change (LUCC) on terrestrial carbon stocks in China between 2000 and 2018, Resour., Conserv. Recycl. 182 (2022) 106333.
[7] A.M. Dewan, Y. Yamaguchi, Land use and land cover change in Greater Dhaka, Bangladesh: using remote sensing to promote sustainable urbanization, Appl. Geogr. 29 (3) (2009) 390–401.
[8] L. Charron, L. Hermanutz, Prioritizing boreal forest restoration sites based on disturbance regime, For. Ecol. Manage 361 (2016) 90–98.
[9] R.J. Corner, A.M. Dewan, S. Chakma, Monitoring and prediction of land-use and land-cover (LULC) change. Dhaka megacity: Geospatial Perspectives on urbanisation, Environment and Health, Springer, 2013, pp. 75–97.
[10] H.T. Do, H.C. Zimmer, J.K. Vanclay, J.C. Grant, B.N. Trinh, H.H. Nguyen, J.D. Nichols, Site form classification—a practical tool for guiding site-specific tropical forest landscape restoration and management, Forestry 95 (2) (2022) 261–273.
[11] R.A.N. Galvez, W.T. Tatil, Spatio-temporal modeling of carbon stocks and estimated carbon market value across different land covers in Cagayan de Oro River Basin, Philipp J Sci 154 (2) (2025).
[12] A.R. Hof, A. Zachrisson, L.E. Polvi, Forest restoration: do site selection and restoration practices follow ecological criteria? A case study in Sweden, Forests 12 (8) (2021) 988.
[13] A. Malik, M. Arief, S. Withaningsih, P. Parikesit, Modeling regional aboveground carbon stock dynamics affected by land use and land cover changes, Glob. J. Environ. Sci. Manag. 10 (1) (2023) 1–22.
[14] R.V. Maretto, L.M. Fonseca, N. Jacobs, T.S. Körting, H.N. Bendini, L.L. Parente, Spatio-temporal deep learning approach to map deforestation in amazon rainforest, IEEE Geosci. Remote Sens. Lett. 18 (5) (2020) 771–775.
[15] A.R. Matamanda, N. Chanza, E. Nyamugadza, Q.L. Chinozvina, Land use planning for climate change adaptation in secondary cities: Insights from Chinhoyi, Zimbabwe, in: A.R. Matamanda, J. Chakwizira, K. Chatiza, V. Nel (Eds.), Secondary Cities and Local Governance in Southern Africa, Springer, Cham, Switzerland, 2024, pp. 155–173.
[16] P. Meli, M. Martínez-Ramos, J.M. Rey-Benayas, J. Carabias, Combining ecological, social and technical criteria to select species for forest restoration, Appl. Veg. Sci. 17 (4) (2014) 744–753.
[17] K. Nam, W.-K. Lee, M. Kim, D.-A. Kwak, W.-H. Byun, H. Yu, H. Kwak, T. Kwon, J. Sung, D.-J. Chung, Spatio-temporal change in forest cover and carbon storage considering actual and potential forest cover in South Korea, Sci. China Life Sci. 58 (7) (2015) 713–723.
[18] B. Bernal, L.T. Murray, T.R. Pearson, Global carbon dioxide removal rates from forest landscape restoration activities, Carbon. Balance Manage 13 (1) (2018) 22.
[19] X. Jiang, A.D. Ziegler, S. Liang, D. Wang, Z. Zeng, Forest restoration potential in China: implications for carbon capture, J. Remote Sens. 2022 (2022) 0006.
[20] Z. Du, L. Yu, J. Yang, D. Coomes, K. Kanniah, H. Fu, P. Gong, Mapping annual global forest gain from 1983 to 2021 with Landsat imagery, IEEe J. Sel. Top. Appl. Earth. Obs. Remote Sens. 16 (2023) 4195–4204.
[21] V. Ouedraogo, K.O. Hackman, M. Thiel, J. Dukiya, Intensity analysis for urban land use/land cover dynamics characterization of Ouagadougou and Bobo-Dioulasso in Burkina Faso, Land. (Basel) 12 (5) (2023) 1063.
[22] S. Natozo, Impact of Urbanization on Housing Conditions in Uganda: a Case Study of Mbale Municipality, 2017.
[23] W. Qi, H. Li, Q. Zhang, K. Zhang, Forest restoration efforts drive changes in land-use/land-cover and water-related ecosystem services in China's Han River basin, Ecol. Eng. 126 (2019) 64–73.
[24] Y. Zhang, K. Cheng, Z. Yang, Y. Chen, H. Yang, Y. Ren, J. Wan, Q. Guo, Spatio-temporal dynamics of future aboveground carbon stocks in natural forests of China, For. Ecosyst. 13 (2025) 100293.
[25] Y. Zhang, Z. Hu, J. Han, X. Liu, Z. Feng, X. Zhang, Spatiotemporal relationship between ecological restoration space and ecosystem services in the Yellow River Basin, China, Land. (Basel) 12 (4) (2023) 730.
[26] F. Röser, O. Widerberg, N. Höhne, T. Day, Ambition in the making: analysing the preparation and implementation process of the Nationally Determined Contributions under the Paris Agreement, Clim. Policy. 20 (4) (2020) 415–429.
[27] F.O. Akinyemi, Land change in the central Albertine rift: insights from analysis and mapping of land use-land cover change in north-western Rwanda, Appl. Geogr. 87 (2017) 127–138.
[28] C. Li, M. Yang, Z. Li, B. Wang, How will Rwandan land use/land cover change under high population pressure and changing climate? Appl. Sci. 11 (12) (2021) 5376.
[29] Mlotha, M.J. (2018). Analysis of land use/land cover change impacts upon ecosystem services in montane tropical forest of Rwanda: forest carbon assessment and REDD+ preparedness.
[30] K. Khan, J.A. Khan, M.F. Khokhar, S.N. Khan, J. Iqbal, Estimating afforestation related forest cover change using data fusion and machine learning, Environ. Res. Commun. 6 (11) (2024) 115004.
[31] N.T. Mukomberanwa, H.K. Madamombe, P. Taru, B. Utete, Modeling urban growth and future scenario projections for Chinhoyi, Zimbabwe using Cellular Automata, J. Earth Environ. Sci. Res. 223 (7) (2025) 2–9, https://doi.org/10.47363/JEESR/2025. *SRC/JEESR-316.*
[32] J.J. Schulz, B. Schröder, Identifying suitable multifunctional restoration areas for forest landscape restoration in Central Chile, Ecosphere 8 (1) (2017) e01644.
[33] S. Sonawane, N.N. Patil, A review of pre-processing techniques. Data engineering and applications, in: Proceedings of the International Conference, IDEA 2K22 1, 2024. Volume.
[34] X. Xu, W. Li, Q. Ran, Q. Du, L. Gao, B. Zhang, Multisource remote sensing data classification based on convolutional neural network, IEEE Trans. Geosci. Remote Sens. 56 (2) (2017) 937–949.
[35] N.T. Mukomberanwa, P. Taru, B. Utete, P. Ngorima, H.K. Madamombe, Landscape connectivity modelling for the African Savannah elephant with spatial absorbing Markov chain and predicting the regenerative power of the range in a mesic protected area, Afr. J. Ecol. 63 (2) (2025) e70034.
[36] A.R. Matamanda, S.H. Mafuku, J.I. Bhanye, The potential of Chinhoyi as a fast-growing secondary city in addressing urban challenges in Zimbabwe, J. Asian Afr. Stud. 59 (5) (2024) 1408–1425.
[37] M.C. Hansen, S.V. Stehman, P.V. Potapov, Quantification of global gross forest cover loss, Proc. Natl. Acad. Sci. USA 107 (19) (2010) 8650–8655.
[38] P.R. Coppin, M.E. Bauer, Digital change detection in forest ecosystems with remote sensing imagery, Rem. Sens. Rev. 13 (3–4) (1996) 207–234.
[39] D. Ziskin, K. Baugh, F.C. Hsu, T. Ghosh, C. Elvidge, Methods used for the 2006 radiance lights, Proc. Asia-Pac. Adv. Netw. 30 (2010) 131, 0.
[40] T.M. Lillesand, R.W. Kiefer. Remote Sensing and Image Interpretation, 3rd, John Wiley & Sons, New York, NY, USA, 1994.
[41] S. Singh, R. Talwar, A comparative study on change vector analysis based change detection techniques, Sadhana 39 (6) (2014) 1311–1331.
[42] A. Singh, Review article digital change detection techniques using remotely-sensed data, Int. J. Remote Sens. 10 (6) (1989) 989–1003.
[43] J.B. Collins, C.E. Woodcock, An assessment of several linear change detection techniques for mapping forest mortality using multitemporal Landsat TM data, Remote Sens. Environ. 56 (1) (1996) 66–77.
[44] R.W. Saaty, The analytic hierarchy process—what it is and how it is used, J. Math. Model. 9 (3–5) (1987) 161–176.

[45] T.L. Saaty, Decision making with the analytic hierarchy process, Int. J. Serv. Sci. 1 (1) (2008) 83.
[46] O.S. Vaidya, S. Kumar, Analytic hierarchy process: an overview of applications, Eur. J. Oper Res. 169 (1) (2006) 1–29.
[47] B.F. Frimpong, F. Molkenthin, Tracking urban expansion using random forests for the classification of landsat imagery (1986–2015) and predicting urban/built-up areas for 2025: a study of the Kumasi metropolis, Land (Basel) 10 (1) (2021) 44.
[48] A. Rajamanickam, C. Kamalakannan, Land use and Land cover prediction in Tamilnadu of India, using random forest machine learning technique, Curr. World Environ. 20 (1) (2025) 206–220.
[49] D.M. Kucuker, O. Tuyoglu, Spatiotemporal patterns and driving factors of carbon dynamics in forest ecosystems: a case study from Turkey, Integr. Environ. Assess. Manage 18 (1) (2021) 209–223.
[50] L. Tian, Y. Tao, W. Fu, T. Li, F. Ren, M. Li, Dynamic simulation of land use/cover change and assessment of forest ecosystem carbon storage under climate change scenarios in Guangdong Province, China, Remote Sens. (Basel) 14 (10) (2022) 2330.
[51] J. Kilama Luwa, Y. Bamutaze, J.-G. Majaliwa Mwanjalolo, D. Waiswa, P. Pilesjö, E.B. Mukengere, Impacts of land use and land cover change in response to different driving forces in Uganda: evidence from a review, Afr. Geogr. Rev. 40 (4) (2021) 378–394.
[52] B.S. Ngoran, S.D. Ngoran, Urban agriculture and landscape challenges in African cities: an illustration of the Bamenda City Council, Cameroon, J. Poverty, Invest. Dev. 15 (2015) 55–72.
[53] S.O. Obiero, Application of GIS and remote sensing methods in land use and land cover change detection: A case study of Kisumu East. Master's Thesis, University of Nairobi, Nairobi, Kenya, 2022.
[54] F. Lesniewska, UNFCCC REDD+ COP Decisions: the cumulative effect on forest related law processes, Int. Commun. Law Rev. 15 (1) (2013) 103–121.
[55] A. Milkias, T. Toru, Assessment of land use land cover change drivers and its impacts on above ground biomass and regenerations of woody plants: a case study at Dire Dawa administration, Ethiopia, Atmos. Clim. Sci. 08 (01) (2018) 111–120.
[56] S. Hermhuk, A. Chaiyes, S. Thinkampheang, N. Danrad, D. Marod, Land use and above-ground biomass changes in a mountain ecosystem, northern Thailand, J. For. Res. (Harbin) 31 (5) (2020) 1733–1742.
[57] R. Leemans, A. van Amstel, C. Battjes, E. Kreileman, S. Toet, The land cover and carbon cycle consequences of large-scale utilizations of biomass as an energy source, Global Environ. Change 6 (4) (1996) 335–357.
[58] E. Eremchenko, Digital Earth: the geospatial revolution and its worldview implications, Philos. Lit. J. Logos 33 (1) (2023) 221–240.
[59] H. Guo, L. Wang, F. Chen, D. Liang, Scientific big data and digital earth, Chin. Sci. Bull. 59 (35) (2014) 5066–5073.